CRYSTAL GROWTH & DESIGN

pubs.acs.org/crystal

Article

Crystal and Molecular Structure of Guaiazulene and Its Potassium Crown Ether Salt: A Conglomerate

Published as part of Crystal Growth & Design special issue "Celebrating the 25th Anniversary of Crystal Growth and Design".

Ivan Bernal, Roger A. Lalancette,* Skye Fortier, Manual Saucedo-Canas, and Pavel Kucheryavy

Cite This: *Cryst. Growth Des.* 2025, 25, 4178–4184

Read Online

ACCESS | Metrics & More | Article Recommendations | Supporting Information

ABSTRACT: The Karplus–Fraenkel theory of electron spin densities was put to the test in an early paper on monomeric azulene (±) radical ions by combining cyclic voltammetry and electron spin resonance. The results were then used to make a comparison with the predicted bond-angle variation of the σ–π interaction parameters (Q's). Unfortunately, the structure of the azulene molecule monomer was not known at the time since it is a tightly held dimer. Recently, the mononuclear anion radical of guaiazulene was prepared by some of us, and the data from the synthesis, solution NMR, and crystallographic data were combined into a single coherent unit, comparing all of the relevant observations from the individual experiments. The resulting amalgamation and interpretation of the combined data are presented below.

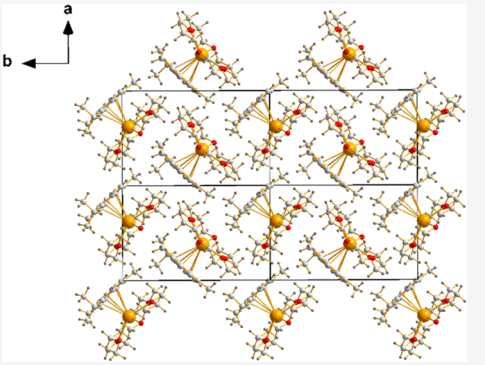

1. INTRODUCTION

A 1962 article on the electrochemical behavior of the nonalternant azulene molecule reported that (a) cyclic voltammetry displays reduction and oxidation waves associated with the transfer, in and out, of one electron each to the neutral moiety,[1] (b) since the voltammetry rate could be adjusted over a broad range, it became clear that the generated (∓) radicals were remarkably stable, and (c) that electron transfer, each way, was reversible (details in the original article[1]). As a result, the electron spin resonance of the anion radical was studied,[1] leading to a complete assignment of the electron spin densities at the five unique hydrogen-bearing carbon sites of the radical anion. A separate study on the electron spin resonance of the *cation* radical was later reported,[2] which was in complete agreement with the information reported in the initial disclosure.[1] Interested readers should read the full report, which also discusses quantum mechanical comparisons of the (∓) pair.[2]

At the time (1962), the ESR results on the anion allowed testing the validity of the so-called Karplus–Fraenkel theory of spin densities, concluding that "*these calculations were used with the experimental splitting constants to make a comparison with the predicted bond-angle variation of the σ-π interaction parameters (Q's). The McLachlan procedure gives much more satisfactory results than the Hückel calculations, but the agreement with the experiment involving the use of the predicted dependence of QCHH on bond angle is only approximate. The theoretical estimates of the variation of QCHH with the bond angle and the constancy of QCCH3H appear to be qualitatively correct. Applications of the theory for the change of QCHH with angle may, in some instances, necessitate taking into account bent bonds.*"[1]

Given that in the 1960s crystal structure determination was slow and primitive, and the structure of azulene as a monomer seemed impossible since the neutral molecule is a tightly held dimer, it is understandable that no further studies were attempted until recently and, if any were tried, none succeeded.

The above comments ignored the fact that the angles used in the quoted publications[1,2] were, at best, approximate, and the conclusions were only qualitative in nature. Moreover, the angles that should be used in the spin density calculations are those for the anion and cation radicals since the ESR measurements are performed on the charged species and not on the neutral molecules. Thus, we have begun a series of structural studies of the ion radicals of selected species, of which the current one is a substituted azulene, the ubiquitous guaiazulene, a choice dictated by the following facts: (a) its superior solubility in convenient solvents, (b) the molecule is a monomer in the solid and in solution, and (c) the ease of

Received: December 31, 2024
Revised: May 19, 2025
Accepted: May 20, 2025
Published: June 10, 2025

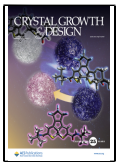

obtaining useful crystals of the neutral molecule from solution and by sublimation.

Until recently, we were unaware that the structure of guaiazulene itself had been determined at 120 K, but it only appears in CCDC[3] as a private communication,[4] without giving further analysis or interpretation of the data. As such, the structure reported is characterized by the properties briefly listed in ref 4. We examined both the guaiazulene (**I**) over the temperature range of 100−296 K and the crown ether salt of azulene at 100 K (**II**). The crystal data for these two structures at 100 K are presented in Table T1 in Supporting information.

2. EXPERIMENTAL SECTION

2.1. Synthesis of Both Guaiazulene and [(18-Crown-6)K(η^5-$C_{15}H_8$)]. A 20 mL scintillation vial was loaded with guaiazulene (250.7 mg, 1.26 mmol), 18-crown-6 (333.4 mg, 1.26 mmol), and THF (7 mL), forming a deep blue solution. To the stirring solution, freshly cut metallic potassium (50.5 mg, 1.29 mmol) was added, and a gradual color change to red-orange was observed along with consumption of the metal over a period of 1.5 h. The mixture was filtered through a Celite column (2 × 0.5 cm^2) supported on glass wool to give an orange filtrate. All volatiles were removed *in vacuo*, and a red-orange powder was obtained. Yield 613.5 mg, 96%. The material was redissolved in THF (5 mL) and stored at −25 °C, giving orange block crystals after 2 days. All air and moisture-sensitive operations were performed in an M. Braun drybox under an atmosphere of purified nitrogen or using high vacuum standard Schlenk techniques. The THF was dried using a Pure Process Technology Solvent Purification System and subsequently stored under a nitrogen atmosphere over activated 4 Å molecular sieves. A sample of guaiazulene was prepared and sent in a vial, and upon examining the contents, crystals suitable for SCXRD were found. 18-Crown-6 was purchased from Oakwood Products, Inc., and made anhydrous using the Gokel method.[5] $[NBu_4][BArF_{24}]$ was synthesized following literature procedures.[6,7] Ultraviolet−visible (UV−vis)/NIR spectra were recorded on a Cary 5000 spectrophotometer. These spectra are shown in the Supporting Information, Figures S1 and S2. UV−vis (THF, 0.11 M, 25 °C, nm, ε = $L{\cdot}mol^{-1}{\cdot}cm^{-1}$): 290 ($\varepsilon$ = 22,528), 304 (ε = 10,350), 335 (ε = 6,471), 366 (ε = 3,620), 435 (ε = 762). NIR (THF, 0.11 M, 25 °C, nm, ε = $L{\cdot}mol^{-1}{\cdot}cm^{-1}$): 853 ($\varepsilon$ = 16), 909 (ε = 16), 977 (ε = 13), 1042 (ε = 12), 1181 (ε = 5), 1258 (ε = 4), 1380 (ε = 2).

2.2. Cyclic Voltammetry. Cyclic voltammetric measurements were performed using a CH Instruments 600E potentiostat with a PC unit controlled with CHI software (version 23.01). Experiments were performed in a glovebox under an inert N_2 atmosphere using platinum disks (2 mm diameter) embedded in Kel-F thermoplastic as both the counter and working electrodes, while the reference electrode consisted of a platinum wire. Solutions utilized in the electrochemical studies were approximately 1 mM in guaiazulene with $[NBu_4][BArF_{24}]$ (0.1M, THF) as the supporting electrolyte. All potentials are reported versus the $[Cp_2Fe]^{0/+}$ couple, referenced as the internal standard.

The cyclic voltammogram (CV) of guaiazulene (shown in Supporting Information as Figure S3), recorded at 100 mVs^{-1}, displays a reduction event at −2.50 V vs $[Cp_2Fe]^{0/+}$, followed by irreversible oxidation at −2.24 V vs $[Cp_2Fe]^{0/+}$. Variable scan rate experiments of both waves indicate a slow electron transfer, as evidenced by the shift in peak potentials for both events. Analysis of the electron transfer mechanism reveals a linear relationship between peak currents and the square root of the scan rate, suggesting homogeneous electron transfer and ruling out an adsorption-mediated process. The $E_{1/2}$ for the guaiazulene/guaiazulenide redox couple is −2.37 V vs $[Cp_2Fe]^{0/+}$, positioning it as significantly more reducing than cobaltocene (−1.33 V) and decamethylcobaltocene (−1.94 V), and closely comparable to strong reductants such as Na(Hg) (−2.36 V) and potassium in liquid ammonia (−2.38 V).[8]

2.3. NMR. NMR experiments were carried out on a Bruker Avance III HD 500 MHz and a Varian Inova 600 MHz spectrometer equipped with broadband probes. Two samples were prepared: 90% guaiazulene +10% acetone-*d6* by volume (**1**), and diluted guaiazulene in acetone-*d6* (5 mg of guaiazulene in 320 μL of acetone-*d6*) (**2**). For the assignment of the signals in ^1H and ^{13}C NMR spectra, COSY, HSQC, and HMBC experiments were carried out, as described below. For the study of intermolecular interactions in the concentrated sample, a series of NOESY experiments with mixing times ranging between 100 and 700 ms were carried out on both the concentrated and the diluted samples. The $^{13}C-^1H$ HOESY experiment, with a 1.5 s mixing time, was used for qualitative assessment of C−H through-space interactions.

2.3.1. Concentrated Guaiazulene Results (1). ^1H NMR (500 MHz, acetone-*d6*): δ 8.45 (d, J = 2.0 Hz, 1H), 7.81 (d, J = 3.8 Hz, 1H), 7.44 (dd, J = 10.6, 2.0 Hz, 1H), 7.40 (d, J = 3.8 Hz, 1H), 7.03 (d, J = 10.6 Hz, 1H), 3.14 (p, J = 6.9 Hz, 1H), 2.91 (s, 3H), 2.90 (s, 3H), 1.50 (d, J = 6.9 Hz, 6H). ^{13}C NMR (126 MHz, acetone-d6): δ 204.81, 143.89, 139.79, 137.78, 136.86, 136.44, 134.70, 132.99, 125.13, 125.04, 113.13, 38.25, 29.53, 29.38, 29.22, 29.07, 28.92, 24.65, 23.65, 12.74.

2.3.2. Diluted Guaiazulene Results (2). ^1H NMR (600 MHz, acetone-*d6*) δ 8.25 (d, J = 2.0 Hz, 1H), 7.59 (d, J = 3.7 Hz, 1H), 7.48 (dd, J = 10.5, 2.0 Hz, 1H), 7.21 (d, J = 3.7 Hz, 1H), 7.05 (d, J = 10.6 Hz, 1H), 3.17 − 3.07 (m, 1H), 2.80 (s, 3H), 2.63 (s, 3H), 1.35 (d, J = 6.9 Hz, 5H). ^{13}C NMR (151 MHz, acetone-d6): δ 166.33, 144.75, 140.69, 138.27, 137.36, 136.95, 135.56, 133.85, 125.79, 125.76, 113.65, 38.85, 25.01, 24.00, 12.90.

2.3.2.1. Results and Discussion (NMR). Assignments of the signals are shown in Table 1, following the atom numbering shown in Scheme 1. The full assignment tables for both the diluted and concentrated samples can be found in the Supporting Information section.

Table 1. Comparison of Chemical Shift (ppm) for the Same Atom in Both Diluted and Concentrated Samples[a]

diluted Sample (**1**)		concentrated Sample (**2**)	
atom	^1H, chemical shift, ppm	atom	^1H, chemical shift, ppm
H2	8.25	H2	8.45
H6	7.59	H6	7.81
H9	7.48	H9	7.44
H5	7.21	H5	7.40
H10	7.05	H10	7.03
H11	3.12	H11	3.14
H15	2.80	H15	2.91
H14	2.63	H14	2.90
H12, H13	1.35	H12,13	1.50

[a]The chemical shift values for the same protons for diluted and concentrated samples are different due to the agglomeration of the molecules in the concentrated sample, which resembles the arrangement of the molecules in the crystalline form.

The NOESY spectrum for the concentrated sample has several extra cross-peaks at (7.81, 1.50), (7.44, 1.50), (7.40, 1.50), (2.90, 1.50), (1.50, 7.81), (1.50, 7.44), (1.50, 7.40), and (1.50, 2.90), which can be assigned to intermolecular interactions (see Figure 1).

A series of NOESY experiments were performed with mixing times between 100 and 700 ms, and the intensities of the NOE signals for CH3−CH correlations were used for the measurements of the interatomic distances by applying the following equation

$$\frac{\eta_{IS}}{\eta_{IIS}} = \frac{r_{IIS}^{-6}}{r_{IS}^{-6}}$$

where η is the intensity of the signal and r is the interatomic distance. Considering $r(CH_3-CH)$ as 2.49 Å from the average distance between CH and the individual protons in the methyl group, as obtained from the crystal structure, intermolecular proton−proton distances were obtained, and they are presented in Table 2.

https://doi.org/10.1021/acs.cgd.4c01760
Cryst. Growth Des. 2025, 25, 4178−4184

Scheme 1. Atom Numbering for Guaiazulene Molecule

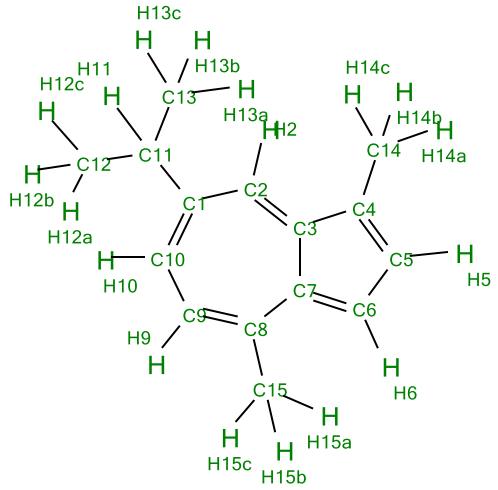

Additionally, an $^{13}C-^{1}H$ HOESY experiment was performed for qualitative assessments of C−H through-space interactions. That spectrum gave a cross-peak at 24.89 (^{13}C), 2.85 (^{1}H), corresponding to the C14/15 − H12/13 through-space correlations, which is shown in Figure 2.

These results for the concentrated sample confirm that the molecules are arranged in a very similar way as described for the crystalline form; i.e., the distances are relatively the same as those found in the SCXRD data. Table 3 gives the intermolecular H···C distances measured by the SCXRD.

2.4. SCXRD Studies of Guaiazulene (I) and the K Crown Ether Complex of Azulene (II). Data for both guaiazulene, $C_{15}H_{18}$, (**I**), and the K crown ether complex of azulene, $C_{27}H_{42}KO_6$, (**II**), were collected on a Rigaku XtaLAB Synergy-S Dual Source diffractometer equipped with a PhotonJet Cu-microfocus source (λ = 1.54178 Å) and a HyPix-6000HE detector. For (**I**), a complete data set was collected at 100 K, and the cell dimensions were checked at 175, 250, and 296 K. For (**II**), data were collected at 100 K, and the cell was checked at 296 K to see that it remained the same. Data reductions were performed with CrysAlisPro65;[9] subsequent data processing was also performed in CrysAlisPro. Using the SCALE3 ABSPACK scaling algorithm66, empirical absorption corrections were applied to the data. Empirical and numerical (Gaussian) absorption corrections, determined by face-indexing and integration, were applied to the data.[9] The structures were solved by applying the intrinsic phasing in SHELXT and refined by full-matrix least-squares techniques against F^2 (SHELXL) in the Olex2 graphical user interface.[10] Anisotropic thermal factors were applied for all atoms except for hydrogen atoms. H atoms were placed in idealized positions and refined using a riding model.[11,12]

The crystal data, intensity data collection, and structure refinement details for both (**I**) and (**II**) are summarized in Table T1 in the Supporting Information. X-ray data for (**I**) and (**II**) have been deposited in the CCDC as #2379905 and #2379903, respectively (see T1). All of the following discussions are based on the parameters from the 100 K data for both structures.

3. RESULTS AND DISCUSSION

3.1. Structure of the Neutral Molecule Guaiazulene (I). At first sight, a description of the structure of guaiazulene should be straightforward since the additional aliphatic side chains separate the components of the dipolar dimer of the parent molecule; however, the solid-state structure still shows some residual interactions described below, meriting comparison with the observations in solution (NMR).

Figures 3 and 4 depict the guaiazulene molecule (**I**), which crystallizes in the orthorhombic space group *Pbca* with Z' = 1.

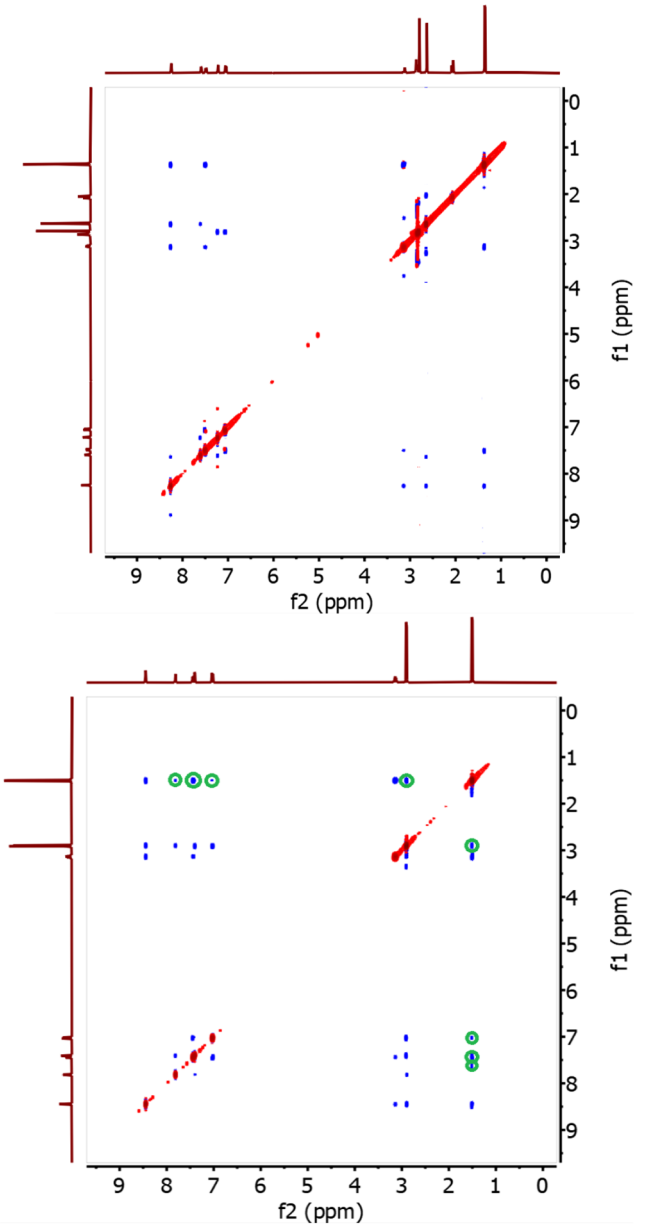

Figure 1. NOESY spectra for diluted (top) and concentrated (bottom) guaiazulene samples. The green circles highlight intermolecular interactions.

The reason for depicting a pair of molecules in Figure 3 is to show what appears to be pairwise interactions between the components in two different ways: short hydrogen−carbon interactions and $\pi-\pi$ carbon−carbon ones. Although this structure has been published before as DEZDAR,[4] it was only determined at 120 K. Since we were interested in establishing whether there were any polymorphic changes vs T, we determined the structure in the range of 100 K through 296 K, which includes the 120 K point. The results are completely compatible. An ORTEP diagram of this molecule is found in the SI as S4.

In this view, there are interesting contacts between adjacent pairs of molecules belonging to the following categories: H−C and C−C, such as

H5···C1A* 3.937 Å C5···C1A* 4.022(2) Å
H6···C2A* 3.022 Å C6···C2A* 3.721(2) Å

https://doi.org/10.1021/acs.cgd.4c01760
Cryst. Growth Des. 2025, 25, 4178−4184

Table 2. Interatomic Distances for Intermolecular Interactions Obtained from the NOESY Experiments Compared to Those from the SCXRD Structure (as Shown Below in Figure 3.)

NOESY (NMR)		XRD	
H6−H12	4.4(2) Å	H6-H12A (8635)[a] 4.466 Å	
H9−H12	3.13(3) Å	H9- H12C (2666) 3.28 Å	
H5−H12	4.21(10) Å	H5- H12C (6565) 2.63 Å	
H12/13-H14/15	3.65(18) Å	H12C- H15B (7456) 3.634 Å	
		H12B- H14B (3565) 2.929 Å	H12C- H14B (6566) 2.734 Å
		H12A- H14B (6566) 2.685 Å	H13A- H15A (1565) 2.834 Å
		H12A- H15B (7456) 2.688 Å	H13B- H15A (1565) 2.872 Å
		H12B- H15B (7456) 3.307 Å	H13B- H14A (8665) 3.709 Å
		H14C- H15C (5655) 3.192 Å	H14C- H14A (8665) 3.132 Å

[a]The numbers in parentheses are the symmetry codes given here: (8635) = 1/2 − x,−5/2 + y,z; (2666) = 1 − x,1 − y,1 − z; (6565) = x,1/2 − y,−1/2 + z; (6566) = x,1/2 − y,1/2 + z; (7456) = −1/2 + x,1/2 − y,1 − z; (5655) = −x + 1,1/2 + y,1/2 − z; (3565) = 1/2 − x,1 − y,1/2 + z; (1565) = x,1 + y,z; (8665) = 1/2 − x,1/2 + y,z. Note that some of these intermolecular contacts (from NOESY) are very close to the ones found from the SCXRD.

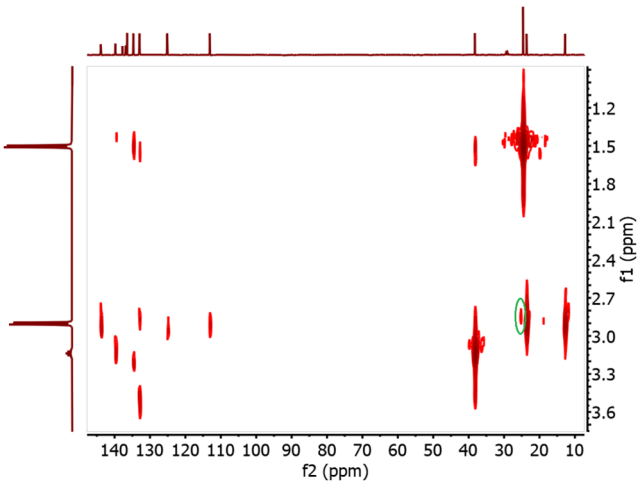

Figure 2. $^{13}C-^{1}H$ HOESY spectrum. The through-space correlation for C14/15 − H12/13 is highlighted by a green ellipse.

Table 3. Intermolecular H···C Distances Measured by SCXRD (in Å)

H2···C6[a] 3.442	H2···C5[a] 3.086	H2···C4[a] 3.406	H11···C4[a] 2.950
H11···C7[a] 2.907	H11···C3[a] 2.673	H15C···C14[b] 3.338	

[a]symm [1/2 − x, 1/2 + y, z]. [b]symm [1/2 + x, y, 1/2 − z].

where * is symm = [1 − x, −1/2 + y, 1/2 − z]

Janiak[13] analyzed the criteria for meaningful π−π "interactions" between aromatic fragments, which, though primarily for heteronitrogen hydrocarbons, is a useful guide for other types. He suggested that given the experimental data then available (see Figure 7 and relevant commentary in his paper),

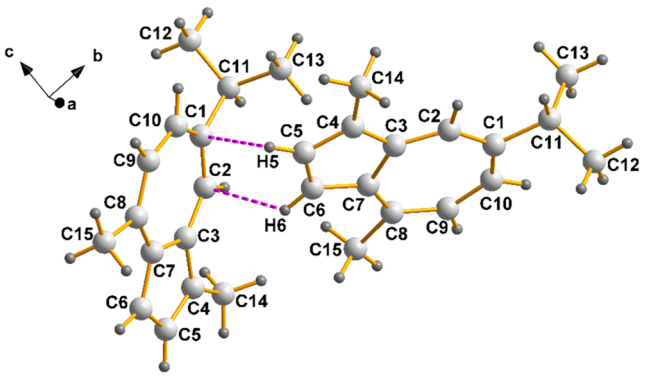

Figure 3. Molecule guaiazulene (I) with its labeling system. The dotted lines show some close H···C contacts present in the polymorph studied here.

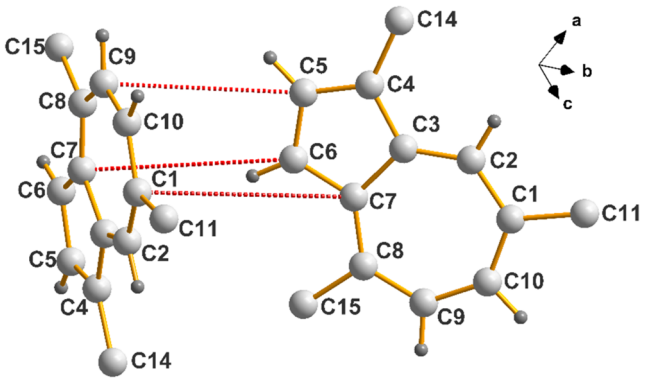

Figure 4. Best projection to illustrate the (five-membered ring)−(seven-membered ring) π−π interaction. The planes of the rings are obviously canted, and the normal between the seven-membered ring (C1, C2, C3, C7, C8, C9, C10) and the five-membered ring (C3, C4, C5, C6, C7) [symm = 1 − x, 1/2 + y, 1/2 - z] is 51.38 °.

the range of 3.3−3.8 Å is reasonable. Figure 4 depicts the close contacts found in guaiazulene.

For numerical values of the above contacts

C5···C9A* = 3.916(2) Å, C6···C7A* = 4.3185(19) Å, C7···C1A* = 4.5337(19) Å, where * is symm = [1 − x, −1/2 + y, 1/2 − z].

Interestingly, the negative five-ring to positive seven-ring interaction still persists. So, aside from the usual π−π contacts expected in molecules such as benzene, naphthalene, etc., in the case of an azulene skeleton, there is still an attractive component that is of the dipolar character.

As pointed out above and documented many times in CSD,[3] the neutral parent azulene is a very tightly held dimer in which the negatively charged five-carbon fragment sits atop the positively charged seven-membered ring, and vice versa.

3.2. Structure of the Potassium Crown Ether Salt of Azulene [(18-Crown-6)K(η^5-$C_{15}H_8$)] (II). A final study of the ESR of azulene is needed, in which all of the ingredients for a proper understanding of the anion and the cation radicals are properly used to correctly determine the Q value discussed above. This is not because the ESR measurements published[1,2] need to be redetermined (those are very precise and final); the problem lies in producing the REAL angular values of the ion radicals without unwanted perturbations on them. The meaning here is the solution studies for the anion were done using a compensating tetra-t-butyl ammonium cation to avoid cation−anion perturbations on the hyperfine splitting measure-

https://doi.org/10.1021/acs.cgd.4c01760
Cryst. Growth Des. 2025, 25, 4178−4184

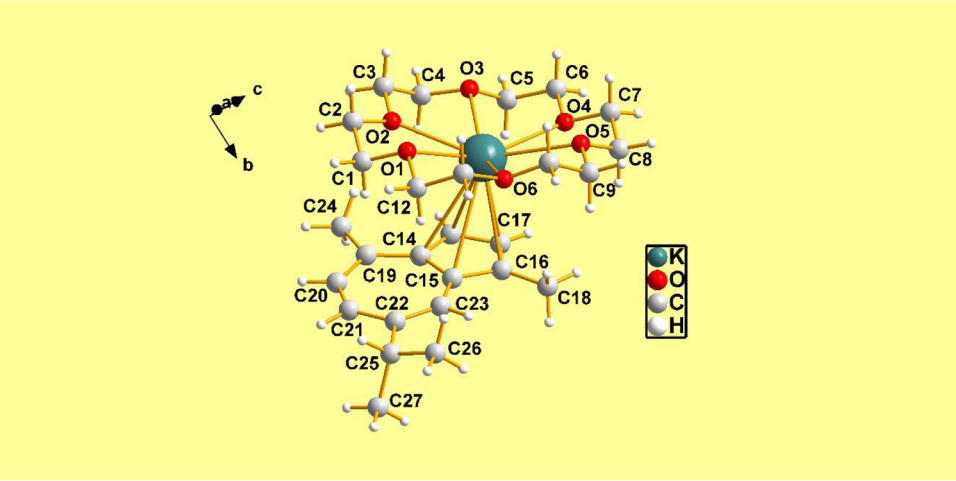

Figure 5. View of the ion pair with the numerical system used in this study. Not surprisingly, the potassium ion sits directly over the five-membered ring at distances of: K−C13 = 3.132(3); K−C14 = 3.367(3); K−C15 = 3.371(3); K−C16 = 3.143(3); K−C17 = 3.012(3) Å (note: C13 atom in the 5-membered ring is not labeled).

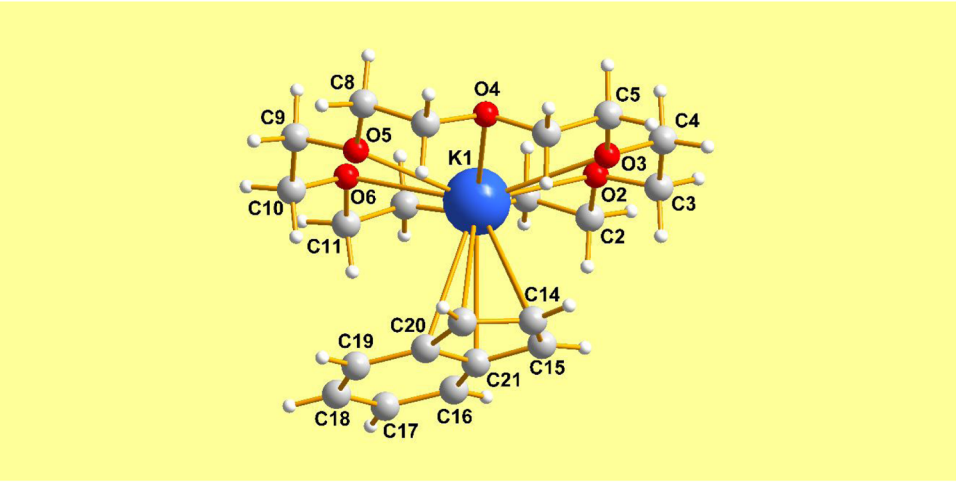

Figure 6. Note that, within stated esd,s, the five-membered rings are the same, despite the differences between indenyl (here) and the azulene present in the crown ether complex (**II**).

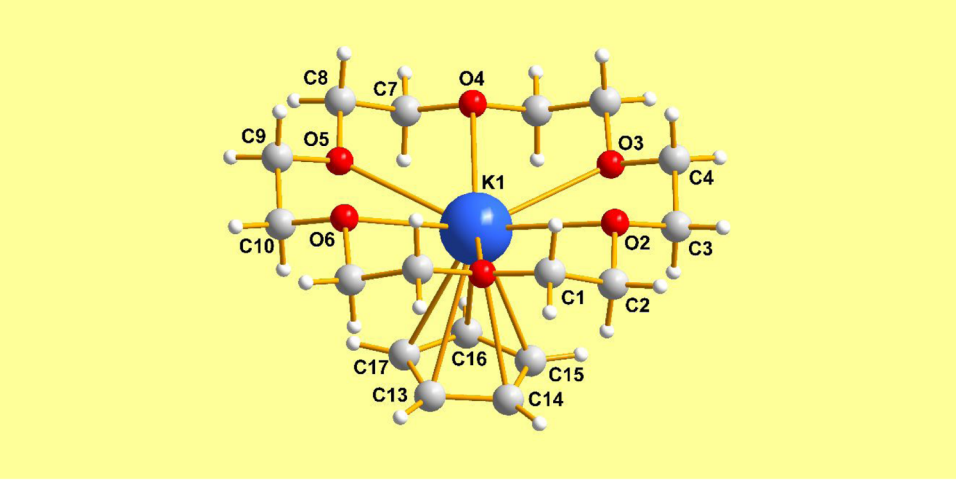

Figure 7. This looks very much like the coordination in Figures 5 and 6 but with bare cyclopentadiene as the ligand.

ments. Consequently, the structure should be determined using that cation—not the alkali metals (like our potassium ether complex). This is likewise true for the cation radicals when and if that structural work is done. We are currently

https://doi.org/10.1021/acs.cgd.4c01760
Cryst. Growth Des. 2025, 25, 4178−4184

engaged in such an attempt. Likewise, we are interested in trying to determine the structures of the cation and anion of azulene itself in its unsubstituted form.

(a) The space group for (**II**) is $P2_1$, $Z = 2.0$, $Z' = 1.0$, which means that the substance crystallized as a conglomerate (e.g., commonly and incorrectly, referred to as "that it spontaneously resolved"). As was mentioned in the synthetic part 2.1 (Synthesis of [(18-crown-6)K(η^5-$C_{15}H_8$)]), the reduction was carried out in the presence of 18-crown-6 that traps the resulting potassium cation that, in turn, becomes the charge-compensating partner for the monoanion of guaiazulene. The molecule (**II**) is shown in Figure 5, above; also, an ORTEP diagram is shown in the SI as S5.

(b) Also, in Figure 6 above, in the structure of BIQMUJ,[14] (1,4,7,10,13,16-hexaoxacyclo-octadecane)-(h^5-indenyl)-(potassium), a very similar potassium cation sits on top of the five-membered ring of an unsubstituted indenyl.

(c) The potassium crown species is π-bonded to the five-membered ring, which is not surprising since it is the negative end of all azulenes; and potassium cations π-bonded to cyclopentadienide-type ligands are documented, as in the case of BIQMIX01,[15] as shown above in Figure 7

The K-carbon distances shown above are

this work (**II**)	BIQMUJ[14]	BIQMIX01[15]
K − C13 3.132(3) Å	K − C13 3.114 Å	K − C13 3.125 Å
K − C14 3.367(3) Å	K − C14 3.056 Å	K − C14 3.142 Å
K − C15 3.371(3) Å	K − C15 3.086 Å	K − C15 3.044 Å
K − C16 3.143(3) Å	K − C20 3.153 Å	K − C16 2.956 Å
K − C17 3.012(3) Å	K − C21 3.122 Å	K − C17 3.009 Å
AVERAGE: 3.205 Å	3.105 Å	3.055 Å

Not surprisingly, this trend suggests that the distance between the K ion and the 5-membered ring gets longer on average as the 5-membered ring gets more substituted.

Comparison of C−C−C angles in the 5-membered cyclopentadiene rings in (**II**), BIQMUJ,[14] and BIQMIX01.[15]

this work (**II**)	BIQMUJ[14]	BIQMIX01[15]
C13−C14−C15 107.15 °	108.88 °	108.20 °
C14−C15−C16 107.21 °	107.72 °	108.04 °
C15−C16−C17 108.09 °	107.52 °	108.01 °
C16−C17−C13 108.31 °	107.21 °	108.00 °
C17−C13−C14 108.22 °	107.66 °	107.75 °
AVERAGE: 107.80 °	107.80 °	108.00 °

These results indicate that the 5-membered ring in the guaiazulene complexed to the potassium crown ether is the same as either of the other two shown above.

4. CONCLUSIONS

Herein, we describe the crystallization and structural characteristics of both guaiazulene and the potassium crown ether complex of azulene itself. All SCXRD information for these two structures can be found in Supporting Table S1. As pointed out above, a final study of the ESR of the monomer of azulene is needed, in which all of the ingredients for a proper understanding of the anion and the cation radicals are properly used to correctly determine the Q values discussed above. This is not because the ESR measurements previously published[1,2] need to be redetermined (those are very precise and final); the problem lies in producing the REAL angular values of the ion radicals without unwanted perturbations on them, such as the presence of alkali metal cations. NOESY and HOESY studies are in agreement with SCXRD, confirming that the arrangement of the molecules in a concentrated solution is similar to that in the crystal structure. For the diluted solution, NMR experiments reveal only intramolecular interactions. A comparison of the azulene complex as its K salt shows that the cation is always centrally bonded to the 5-membered ring system and that the K−C bond distances (in the cyclopentadiene) get larger as the substitutions on that ring get more pronounced.

■ ASSOCIATED CONTENT

Supporting Information

The Supporting Information is available free of charge at https://pubs.acs.org/doi/10.1021/acs.cgd.4c01760.

The contents are for the NMR data for diluted guaiazulene; ^{13}C NMR; COSY; HSQC; HMBC; assignment Table; concentrated Guaiazulene; ^{13}C NMR; COSY; HSQC; HMBC; assignment Table. The following files are available free of charge: CIF and CheckCIF files for guaiazulene (**I**) CIF and CheckCIF files for K etherate salt of guaiazulene (**II**) (PDF)

Accession Codes

Deposition Numbers 2379903 and 2379905 contain the supplementary crystallographic data for this paper. These data can be obtained free of charge via the joint Cambridge Crystallographic Data Centre (CCDC) and Fachinformationszentrum Karlsruhe Access Structures service.

■ AUTHOR INFORMATION

Corresponding Author

Roger A. Lalancette − *Carl A. Olson Memorial Laboratories, Department of Chemistry, Rutgers University, 07102 Newark, New Jersey, United States;* orcid.org/0000-0002-3470-532X; Email: roger.lalancette@gmail.com

Authors

Ivan Bernal − *Carl A. Olson Memorial Laboratories, Department of Chemistry, Rutgers University, 07102 Newark, New Jersey, United States; Molecular Sciences Institute, School of Chemistry, University of the Witwatersrand, 2050 Johannesburg, South Africa*

Skye Fortier − *University of Texas at El Paso, Department of Chemistry, 79968 El Paso, Texas, United States;* orcid.org/0000-0002-0502-5229

Manual Saucedo-Canas − *University of Texas at El Paso, Department of Chemistry, 79968 El Paso, Texas, United States*

Pavel Kucheryavy − *Carl A. Olson Memorial Laboratories, Department of Chemistry, Rutgers University, 07102 Newark, New Jersey, United States*

Complete contact information is available at: https://pubs.acs.org/10.1021/acs.cgd.4c01760

Author Contributions

This manuscript was written through contributions of all authors. All authors have given approval to the final version of the manuscript.

Funding

S.F. is grateful to the Welch Foundation (AH-1922−20230405) for support of this work. There were no other outside funding sources used to support this research.

Notes

The authors declare no competing financial interest.

■ ACKNOWLEDGMENTS

The X-ray diffractometer used in these studies at Rutgers University was purchased with support from the NSF and Rutgers University, grant 2018753. S.F. is grateful to the Welch Foundation (AH-1922-20230405) for support of this work and to the NSF for providing funding for the purchase of an X-ray diffractometer (CHE-1827875).

■ REFERENCES

(1) Bernal, I.; Rieger, P. H.; Fraenkel, G. K. ESR of Azulene Anion Radical. *J. Chem. Phys.* **1962**, *37*, 1489−1495.
(2) Dessau, R. M.; Shih, S. Electron Spin Resonance of Azulene Radical Cations. *J. Chem. Phys.* **1970**, *53*, 3169−3172.
(3) Groom, C. R.; Bruno, I. J.; Lightfoot, M. P.; Ward, S. C. The Cambridge Structural Database. *Acta Crystallogr., Sect. B: Struct. Sci., Cryst. Eng. Mater.* **2016**, *72*, 171−179.
(4) Nakai, M.; Miki, K.; Kaga, A.; Yamano, M. CSD, Private Communication CCDC 2251405. Crystallographic Details: Sp. Gr. = Pbca, a = 14.3270(9), b = 9.7222(6), c = 16.9757(13), V = 2364.5(3). 2283 data at T = 119.99(10) K, R = 6.07. 2023.
(5) Gokel, G. W.; Cram, D. J.; Liotta, C. L.; Harris, H. P.; Cook, F. L. Preparation and purification of 18-crown-6[1,4,7,10,13−16-hexaoxacyclooctadecane]. *J. Org. Chem.* **1974**, *39*, 2445−2446.
(6) Martínez-Martínez, A. J.; Weller, A. S. Solvent-free anhydrous Li^+, Na^+ and K^+ salts of $[B(3,5\text{-}(CF_3)_2C_6H_3)_4]^-$, $[BAr_4^F]^-$. Improved synthesis and solid-state structures. *Dalton Trans.* **2019**, *48* (11), 3551−3554.
(7) Bartlett, P. N.; Cook, D. C.; George, M. W.; Ke, J.; Levason, W.; Reid, G.; Su, W.; Zhang, W. Phase behaviour and conductivity study on multi-component mixtures for electrodeposition in supercritical fluids. *Phys. Chem. Chem. Phys.* **2010**, *12*, 492−501.
(8) Connelly, N. G.; Geiger, W. E. Organometallic Chemistry. *Chem. Rev.* **1996**, *96* (2), 877−910.
(9) Rigaku Oxford Diffraction. *CrysAlisPro Software system, version 171.41.27a*; Rigaku Corporation: Oxford, UK, 2019.
(10) Dolomanov, O. V.; Bourhis, L. J.; Gildea, R. J.; Howard, J. A. K.; Puschmann, H. J. *OLEX2*: a complete structure solution, refinement and analysis program. *J. Appl. Cryst.* **2009**, *42*, 339−341.
(11) Sheldrick, G. M. Crystal structure refinement with SHELXL. *Acta Crystallogr., Sect. C: Struct. Chem.* **2015**, *71*, 3−8.
(12) Sheldrick, G. M. SHELXT − Integrated space-group and crystal-structure determination. *Acta Crystallogr., Sect. A: Found. Adv.* **2015**, *71*, 3−8.
(13) Janiak, C. A critical account on $\pi-\pi$ stacking in metal complexes with aromatic nitrogen-containing ligands. *J. Chem. Soc., Dalton Trans.* **2000**, 3885−3896.
(14) Neander, S.; Tio, F. E.; Buschmann, R.; Behrens, U.; Olbrich, F. Cyclopentadienyl, indenyl, fluorenyl, and pentamethylcyclopentadienyl complexes of potassium with 18-crown-6. *J. Organomet. Chem.* **1999**, *582*, 58−65.
(15) Benda, C. B.; Waibel, M.; Fassler, T. F. On the Formation of Intermetalloid Clusters: Titanocene(III)diammin as a Versatile Reactant Toward Nonastannide Zintl Clusters. *Angew. Chem., Int. Ed.* **2015**, *54*, 522−526.

https://doi.org/10.1021/acs.cgd.4c01760
Cryst. Growth Des. 2025, 25, 4178−4184